Ti location in the MFI framework of Ti-Silicalite-1: a neutron powder diffraction study.

6 AUTHORS, INCLUDING:

Carlo Lamberti
Università degli Studi di Torino
379 PUBLICATIONS **13,103** CITATIONS

SEE PROFILE

A. Zecchina
Università degli Studi di Torino
560 PUBLICATIONS **19,907** CITATIONS

SEE PROFILE

Gilberto Artioli
University of Padova
255 PUBLICATIONS **3,356** CITATIONS

SEE PROFILE

Gianluigi Marra
Istituto ENI Donegani Research Center for No…
61 PUBLICATIONS **980** CITATIONS

SEE PROFILE

Ti Location in the MFI Framework of Ti−Silicalite-1: A Neutron Powder Diffraction Study

Carlo Lamberti,*,†,‡ Silvia Bordiga,† Adriano Zecchina,† Gilberto Artioli,§ Gianluigi Marra,‖ and Guido Spanò‖

Contribution from the Dipartimento di Chimica IFM, Università di Torino, Via P. Giuria 7, 10125 Torino, Italy, INFM Unità di Torino Università, Torino, Italy, Dipartimento di Scienze della Terra, Università di Milano, Via Botticelli 23, I-20133 Milano, Italy, and Centro CNR di Studio per la Geodinamica Alpina e Quaternaria, Via Mangiagalli 34, I-20133 Milano, Italy, and EniChem S.p.A. Centro Ricerche Novara, Istituto G. Donegani, Via G. Fauser 4, I-28100 Novara, Italy

Received October 12, 2000

Abstract: The first direct evidence that Ti atoms are not equally distributed in the 12 crystallographically independent T sites of the MFI framework is presented on the basis of neutron diffraction data collected at the HRPD instrument of the ISIS pulsed neutron source. We found strong evidence indicating that T6, T7, and T11 are the most populated sites and weak evidence that Ti may be hosted in T10. Ti occupancy can be excluded for sites T1, T2, T4, T5, T9, and T12. The occupancy of the remaining sites is doubtful. Since defective silicalite has been shown to exhibit the same preferential sites (T6, T7, T11, and T10) for Si vacancies, it may be suggested that the incorporation mechanism of the Ti atoms in the MFI framework occurs via the insertion of titanium in the defective sites. This hypothesis implies that titanium has a mineralizing effect on the MFI framework, and it is supported by independent spectroscopic data on both TS-1 and defective silicalite. The results are discussed in comparison with the known substitution mechanisms in the T-sites of MFI-type structures.

1. Introduction

Ti−silicalite[1] (TS-1) shows a remarkable high efficiency and molecular selectivity in oxidation reactions employing H_2O_2 under mild conditions such as the conversions of ammonia to hydroxylamine, of secondary alcohols to ketones, and of secondary amines to dialkylhydroxylamines or reactions such as the phenol hydroxylation, the olefin epoxidation, and the cyclohexanone ammoximation.[1−8] For these reasons TS-1 has become one of the most relevant industrial catalysts in the last 20 years. Silicalite, the parent Ti-free material with the same MFI topology, does not show a comparable activity, and therefore, the Ti atoms have been immediately designed as the catalytic centers of the material. The structural nature of Ti atoms in TS-1 has been lively debated in the eighties; titanyl groups, extraframework defect sites, monomeric and dimeric Ti species, and Ti species incorporated in edge-sharing units forming bridges across the zeolite channels have been inferred

by different authors. The same holds for the local geometry, where Ti species having tetrahedral, square pyramidal, or octahedral coordination have been suggested.

The origin of the initial confusion was related to the difficulty encountered in the synthesis of well-manufactured TS-1, which requires the use of extremely pure reagents and careful control in the synthesis conditions.[1] Characterization of imperfectly synthesized samples leads to misinterpretation of structural and spectroscopic data. There is now a large consensus that Ti atoms are incorporated into MFI framework in $[TO_4]$ sites substituting silicon atoms.[9,10] In particular, the model of isomorphous substitution has been put forward on the basis of several independent characterization techniques, namely XRD,[11,12] IR (Raman),[13−17] UV−vis,[17,18] EXAFS, and XANES.[19−25] It has also been shown that the catalytic activity of the Ti site, in several partial oxidation reactions, is related to the fraction of

* To whom correspondence should be addressed: Tel. +39011-6707841. Fax: +39011-6707855. E-mail: lamberti@ch.unito.it.
† Dipartimento di Chimica IFM, Università di Torino.
‡ INFM Unità di Torino.
§ Dipartimento di Scienze della Terra Università di Milano and Centro CNR Milano.
‖ EniChem Novara.

(1) Taramasso, M.; Perego, G.; Notari, B. U.S. Patent No. 4410501, 1983.
(2) Clerici, G. M. *Appl. Catal.* **1991**, *68,* 249.
(3) Clerici, G. M.; Bellussi, G.; Romano, U. *J. Catal.* **1991**, *129,* 159.
(4) Bellussi, G.; Carati, A.; Clerici, G. M.; Maddinelli, G.; Millini, R. *J. Catal.* **1992**, *133,* 220.
(5) Notari, B. *Adv. Catal.* **1996**, *41,* 253 and references therein.
(6) Roffia, P.; Leofanti, G.; Cesana, A.; Mantegazza, M. A.; Padovan, M.; Petrini, G.; Tonti, S.; Gervasutti, P. *Stud. Surf. Sci. Catal*. **1990**, *55,* 543.
(7) Mantegazza, M. A.; Leofanti, G.; Petrini, G.; Padovan, M.; Zecchina, A.; Bordiga, S. *Stud. Surf. Sci. Catal*. **1994**, *82,* 541.
(8) Mantegazza, M. A.; Petrini, G.; Spanò, G.; Bagatin, R.; Rivetti, F. *J. Mol. Catal. A* **1999**, *146,* 223.

(9) Millini, R.; Perego, G. *Gazz. Chim. Ital.* **1996**, *126,* 133.
(10) Vayssilov, G. N. *Catal. Rev.−Sci. Eng.* **1997**, *39,* 209.
(11) Millini, R.; Previdi Massara, E.; Perego, G.; Bellussi, G. *J. Catal.* **1992**, *137,* 497.
(12) Lamberti, C.; Bordiga, S.; Zecchina, A.; Carati, A.; Fitch, A. N.; Artioli, G.; Petrini, G.; Salvalaggio, M.; Marra, G. L. *J. Catal.* **1999**, *183,* 222.
(13) Tozzola, G.; Mantegazza, M. A.; Ranghino, G.; Petrini, G.; Bordiga, S.; Ricchiardi, G.; Lamberti, C.; Zulian, R.; Zecchina, A. *J. Catal.* **1998**, *179,* 64.
(14) Boccuti, M. R.; Rao, K. M.; Zecchina, A.; Leofanti G.; Petrini, G. *Stud. Surf. Sci. Catal.* **1989**, *48*, 133.
(15) Zecchina, A.; Spoto, G.; Bordiga, S.; Padovan, M.; Leofanti, G. *Stud. Surf. Sci. Catal.* **1991**, *65,* 671.
(16) Scarano, D.; Zecchina, A.; Bordiga, S.; Geobaldo, F.; Spoto, G.; Petrini, G.; Leofanti, G.; Padovan, M.; Tozzola, G. *J. Chem. Soc., Faraday Trans.* **1993**, *89,* 4123.
(17) Zecchina, A.; Spoto, G.; Bordiga, S.; Ferrero, A.; Petrini, G.; Padovan, M.; Leofanti, G. *Stud. Surf. Sci. Catal.* **1991**, *69,* 251.
(18) Blasco, T.; Camblor, M.; Corma, A.; Pérez-Parriente, J. *J. Am. Chem. Soc.* **1993**, *115,* 11806.

tetrahedral Ti atoms incorporated in TS-1.[8] Moreover, theoretical studies have shown that the isomorphous insertion of Ti atoms in the zeolitic lattice is energetically favored.[26−30] Although the local geometry of the Ti sites has been satisfactorily clarified, the distribution of the Ti atoms over the 12 symmetry-independent T sites of MFI framework is still open to debate. This is an important problem, since the localization of Ti atoms may play an important role in understanding the catalytic properties of the material.

Unfortunately, the extremely small dimensions of TS-1 crystals do not permit the use of the more informative single-crystal technique, and all direct structural information has been to date derived from powder diffraction. Moreover, the low fraction of Ti atoms that can be inserted into the MFI framework (about 3 TiO_2 wt %)[11] makes the experimental localization of the Ti atoms from X-ray diffraction measurements very difficult. For these reasons the most interesting speculations concerning Ti distribution are to date based on computational chemistry results.[26−34]

The first theoretical contribution to the debate (Jentys and Catlow[26]) used defect energy minimization and quantum mechanical cluster computation to study the isomorphous Ti substitution in monoclinic MFI. The obtained distances are very close to those experimentally found by EXAFS experiments on well-manufactured TS-1 samples.[19−22,24,25] The authors conclude that, among the 24 different T sites, no clear preferential site was emerging from the energy calculation. Millini et al.[27] reached the same conclusion concerning orthorhombic MFI on the basis of local density functional quantum mechanical calculations on pentameric $Ti(OSiO_3H_3)_4$ cluster. The authors of ref 27 used a fixed cluster geometry, closely conforming to the geometry of the MFI framework. By substituting Ti in the 12 different T sites of the orthorhombic cell, they found a relatively small spread of energy and conclude in favor of an homogeneous distribution of the heteroatom. The obtained Ti−O distance (1.80 Å) was in full agreement with EXAFS data.[19,20−22,24,25]

Oumi et al.[31] investigated the isomorphic substitution of Ti into the orthorhombic MFI framework using a molecular dynamics (MD) approach. The interesting result of their work is the claim that the lattice parameter expansion along the three crystallographic axes is related to a specific substituted site. They report the increment of the cell *a*, *b,* and *c* parameters assuming that all Ti atoms are incorporated into a single T site and conclude that only substitution into the T8 site is compatible with the experimentally measured Δ*a*, Δ*b*, and Δ*c* reported by the group of Perego.[11] On the other hand, the possibility of Ti distribution into different sites, resulting in a linear combination of the corresponding Δ*a*, Δ*b*, and Δ*c* values, has not be considered by the authors and the equilibrium Ti−O distance reported by Oumi et al.[31] (1.85 Å) is substantially larger than the experimental value observed by EXAFS.[19−22,24,25] In a subsequent MD work Smirnov and van de Graaf[32] did not found any correlation between the unit cell expansion and the Ti location. More recently, Njo et al.[33] reported a study based on combined Metropolis Monte Carlo and molecular dynamics. Following previous EXAFS results[19,20,21] they adopt a force field where the Ti−O bond is simulated by a harmonic potential with a minimum at 1.80 Å and a force constant of 211 N/m. The authors[33] arbitrarily locate 5 Ti atoms in a double unit cell (effectively approaching the experimental limit of *x* = 0.025; see ref 11) and optimize the lattice geometry and the Ti, Si distribution over 192 T sites (5 Ti and 187 Si) using a MD approach. Each T site distribution is inductively generated from the previous configuration by random exchange of Ti with a Si atom. The new distribution is geometrically optimized and accepted if its energy is lower than that of the previous configuration. If not, its Boltzman probability *w* = exp[Δ*E*/*kT*] is compared with a randomly generated number *n*, where 0 < *n* < 1. If *w* > *n* the new distribution is accepted, otherwise the system returns to the previous Ti, Si distribution. Following this approach, Njo et al.[33] have found T2 and T12 as preferential sites for Ti substitution, while T8 (suggested as preferential site from MD calculation in ref 31) is among the less populated sites. It should also be noted that the lattice expansion Δ*a*, Δ*b*, and Δ*c* computed by MD calculation[31] for Ti insertion in sites T2 and T12 (suggested as preferential sites in ref 33) are not compatible with the experimental values reported by the group of Perego.[11]

Finally, the most recent results obtained by Sauer and co-workers[34] highlight how all previous computational results, performed by simulating the zeolite structure in a vacuum (i.e. without adsorbed water molecules), ought to be considered with caution. The effect of hydration must in fact be considered when discussing insertion of Ti in the framework sites because, in the presence of water, the variations in the site stabilization energy among different Ti substituted T sites are substantially larger (up to 40 kJ mol^{-1}) than in the anhydrous case. The ranking of the substituted T sites on the basis of the computed energy changes extensively if hydration is taken into account.

It is clear that the available theoretical data at present do not provide a definite answer to the problem of the existence of preferential insertion of Ti in the MFI framework and that the experimental evidence is also very limited. [49]Ti and [47]Ti NMR studies[35,36] have been performed, but they are of difficult interpretation because of the large quadrupolar moment of both nuclei. Also ^{29}Si MAS NMR spectroscopy, usually widely employed in the characterization of zeolites because of its

(19) Bordiga, S.; Coluccia, S.; Lamberti, C.; Marchese, L.; Zecchina, A.; Boscherini, F.; Buffa, F.; Genoni, F.; Leofanti, G.; Petrini, G.; Vlaic, G. *J. Phys. Chem.* **1994**, *98,* 4125.

(20) Bordiga, S.; Boscherini, F.; Coluccia, S.; Genoni, F.; Lamberti, C.; Leofanti, G.; Marchese, L.; Petrini, G.; Vlaic, G.; Zecchina, A. *Catal. Lett.* **1994**, *26*, 195.

(21) Pei, S.; Zajac, G. W.; Kaduk, J. A.; Faber, J.; Boyanov, B. I.; Duck, D.; Fazzini, D.; Morrison T. I.; Yang, D. S. *Catal. Lett.* **1993**, *21,* 333.

(22) Le Noc, L.; Trong On, D.; Solomykina, S.; Echchahed, B.; Béland, F.; Cartier dit Moulin, C.; Bonneviot, L. *Stud. Surf. Sci. Catal.* **1996**, *101*, 611.

(23) Zecchina, A.; Bordiga, S.; Lamberti, C.; Ricchiardi, G.; Scarano, D.; Petrini, G.; Leofanti, G.; Mantegazza, M. *Catal. Today* **1996,** *32,* 97.

(24) Lamberti, C.; Bordiga, S.; Arduino, D.; Zecchina, A.; Geobaldo, F.; Spanò, G.; Genoni, F.; Petrini, G.; Carati, A.; Villain, F.; Vlaic, G. *J. Phys. Chem. B* **1992**, *102,* 6382.

(25) Gleeson, D.; Sankar, G.; Catlow, C. R. A.; Thomas, J. M.; Spanó, G.; Bordiga, S.; Zecchina, A.; Lamberti, C. *Phys. Chem. Chem. Phys.* **2000,** *2,* 4812.

(26) Jentys, A.; Catlow, C. R. A. *Catal. Lett.* **1993**, *22*, 251.

(27) Millini, R.; Perego, G.; Seiti, K. *Stud. Surf. Sci. Catal.* **1994,** *84,* 2123.

(28) de Mann, A. J. M.; Sauer, J. *J. Phys. Chem.* **1996**, *100*, 5025.

(29) Sinclair, P. E.; Sankar, G.; Catlow, C. R. A.; Thomas, J. M.; Maschmeyer, T. *J. Phys. Chem. B* **1997***, 101,* 4237. (b) Sinclair, P. E.; Catlow, C. R. A. *J. Phys. Chem. B* **1999***, 103*, 1084.

(30) Zicovich-Wilson, C. M.; Dovesi, R.; Corma, A. *J. Phys. Chem. B* **1999***, 103*, 988.

(31) Oumi, Y.; Matsuba, K.; Kubo, M.; Inui, T.; Miyamoto, A. *Microporous Mater.* **1995***, 4,* 53.

(32) Smirnov, K. S.; van de Graaf, B. *Microporous Mater.* **1996***, 7,* 133.

(33) Njo, S. L.; van Koningsveld, H.; van de Graaf, B. *J. Phys. Chem. B* **1997**, *101*, 10065.

(34) Ricchiardi, G.; de Man, A.; Sauer, J. *Phys. Chem. Chem. Phys.* **2000**, *2*, 2195.

(35) Berger, S.; Bock, W.; Marth, C.; Raguse, B.; Reetz, M. *Magn. Reson. Chem.* **1990**, *28*, 559.

(36) Lopez, A.; Tuilier, M.; Guth, J.; Delmotte, L.; Popa, J. *Solid State Chem.* **1993**, *102*, 480.

sensitivity to the atoms attached to the oxygens of the [SiO$_4$] units, has provided much less information when applied to study the nature of Ti sites in TS-1. In fact, unlike the ZSM-5 zeolite and B-silicalite cases, where Si atoms having one Al or B atom in the second coordination shell ([Si(OSi)$_3$OAl] and [Si-(OSi)$_3$OB]) show well-identified NMR lines, the influence of titanium in the framework position neighboring tetrahedral silicon atoms [Si(OSi)$_3$OTi] results only in a shoulder at about −115 ppm in the ^{29}Si MAS spectrum.[22,37] Moreover, since a similar shoulder was also observed for [Si(OSi)$_3$OH] units in defective silicalite with a high density of Si vacancies,[22,38] an unambiguous assignment in the −115 ppm shoulder in the ^{29}Si MAS NMR spectra to Ti only cannot be done.[22,39] It is in fact worth recalling that TS-1 is a rather defective material, hosting Si vacancies generating internal hydroxyl groups; vide infra section 4.2. In this regard it is worth recalling the contribution of the group of Bonneviot,[22] reporting an ^{1}H MAS NMR attempt to distinguish TiOH groups from SiOH in TS-1. Very recently, Laborian et al.[40] have reported an original ^{29}Si MAS NMR study of different titanosilicates, where Ti^{4+} species have been previously reduced to the paramagnetic Ti^{3+} species by treatment in CO. The Fermi contact interaction between the unpaired electron of Ti^{3+} species and the ^{29}Si nucleus allows one to extract information on titanium; in particular, the authors claim that the reduction of the NMR signal is proportional to the number of paramagnetic Ti^{3+} species.

The results of adsorption microcalorimetry experiments have recently been reported by Bolis et al.[41,42] using NH$_3$ as a probe. They reported that the evolution of the heat of adsorption with coverage of ammonia at the Ti(IV) sites was typical of heterogeneous surfaces. The authors interpreted this result as an indirect evidence that Ti is either randomly distributed among the 12 crystallographically independent T sites of the orthorhombic MFI cell or it is preferentially located in some of the sites, discarding the hypothesis of a single preferred substitutional site.

To provide a definite answer to the problem, we recently reported the attempt to directly locate the Ti atoms using XRPD data collected at the high-resolution powder diffraction beam line (BM16) of the ESRF (European Synchrotron Radiation Facility).[12] The high photon flux emitted by a bending magnet of the ESRF at $\lambda = 0.85018$ Å allowed us to collect high-quality data on a set of different TS-1 samples down to 0.85 Å in d spacing. Our goal was to detect any significant increase of charge density in the T sites, as expected on the basis of the higher Z of Ti with respect to Si ($\Delta Z = 8$). This is possible in principle only if all Ti atoms are partitioned in a single crystallographic site. Different refinement strategies have been adopted in order to reliably recognize a significant titanium occupancy x_i (being that of silicon of the same site constrained to $1 - x_i$: $i = 1$ to 12) in some of the T sites. In some of the samples, a few sites yielded an apparent x_i value significant at the 3σ level or higher (in particular T6 and T11), but it was clear that the resulting x_i value was strategy dependent. This was not surprising, since a correlation between the x_i parameters

and the Si, Ti Debye−Waller factors is always expected. The fact that the probable preferred T sites were found to be different in the different samples, and even in the same sample subject to different thermal treatment, led us to deduce that residual non statistical errors were affecting the data analysis. It was inferred that either high-resolution XRPD is not sensitive enough to identify preferred substituted T sites, because of the insufficient electron density contrast between Si and Ti and the low Ti content, or else Ti is randomly distributed over most of the 12 T sites.

The present work relies on the large contrast existing between the neutron coherent scattering lengths of Ti and Si [b_c(Ti) = −3.438(2) fm; b_c(Si) = +4.149(1) fm] and attempts the location of the Ti atoms in the framework sites of three well-characterized TS-1 samples by high-resolution time-of-flight neutron powder diffraction.

2. Experimental Section

To avoid any bias due to the refinement performed on diffraction data collected on a single sample, two high-Ti-loaded samples prepared in two different syntheses (A and B) were employed (in both cases the original patent[1] has been followed. Template (tetrapropylammonium) removal has been performed by calcinating the samples in air flux up to 550 °C. The successive TGA up to 850 °C do not reveal any measurable trace of organic molecules, indicating that the template decomposition has been virtually complete. In the products of both syntheses the insertion of Ti in the MFI framework was preliminarily checked by IR, UV−vis, and XANES spectroscopy (data are not reported here for brevity). The amount of framework Ti (x) was evaluated by measuring the cell volume and using the following empirical equation:[12] $V = 2093x + 5335.8$ Å^3. The cell volume of the samples dehydrated at 120 °C was extracted by full-profile analysis of XRPD collected on a laboratory Bruker D5005 instrument equipped with Göbel mirrors. The calculated number of incorporated Ti atoms/unit cell were 2.09 and 2.64 for synthesis A and B, respectively. These values are, within the experimental errors, in agreement with the chemical analysis data, reporting 2.06(5) and 2.66(5) Ti atoms/unit cell for samples A and B, respectively. By comparing the cell volume obtained by XRD and elemental analysis data, we conclude that virtually all titanium is to be considered structurally inserted in the framework.

For the neutron measurements, about 3 cm^3 of TS-1 obtained from each synthesis was dehydrated at 120 °C and then sealed in a glass vial under vacuum (hereafter labeled samples A120 and B120). To measure a third set of diffraction data on an independent sample, a further 3 cm^3 of TS-1 obtained from synthesis A has been treated in a vacuum at 500 °C and then sealed in a glass vial (hereafter named sample A500). The three sample vials were successively loaded in the sample holder of the High-Resolution Powder Diffractometer (HRPD) at the Intense Spallation Isotope Source (ISIS), Rutherford Appleton Laboratory, Didcot, U.K. HRPD offers excellent resolution throughout the diffraction pattern ($\Delta d/d \cong (4-5) \times 10^{-4}$). Data were accumulated on each sample at room temperature for about 24 h in order to obtain high-quality statistics. Two ZnS scintillator banks at 168 and 90° with respect to the incident beam were used. The data from the 90° bank were used in the time-of-flight range 35−120 ms (corresponding to the range 1.01−3.45 Å in d space) and those from the 168° bank in the time-of-flight range 43−118 ms (0.88−2.45 Å in d space). The two independently measured powder patterns for each sample were simultaneously analyzed using the full-profile Rietveld method. Detector calibration, source-to-sample distance, and starting peak profile parameters were obtained by careful refinement of the powder diffraction data of reference BaF$_2$ collected using identical experimental conditions.

The goals pursued in this experiment are extremely challenging due to the low concentration of Ti; therefore, a reduction of the thermal contribution to the atomic displacement parameters would be very useful in the detection of any possible preferential substitution site. The experimental temperature therefore ought to be as low as possible, but carefully selected, to avoid the observed orthorhombic to monoclinic phase transition,[43] which implies a decrease in the lattice symmetry, a doubling of the symmetrically independent T sites, and the halving of

(37) Kraushaar, B.; van Hoof, J. H. C. *Catal. Lett.* **1988**, *1*, 81.

(38) Van der Pol, A. J. H. P.; van Hoof, J. H. C. *Appl. Catal. A* **1992**, *92*, 93.

(39) Labourian, A.; Higley, T. J.; Earl, W. L. *J. Phys. Chem. B* **1998**, *102*, 2897.

(40) Labourian, A.; Ott, K. C.; Rau, J.; Earl, W. L. *J. Phys. Chem. B* **2000**, *104*, 5890.

(41) Bolis, V.; Bordiga, S.; Lamberti, C.; Zecchina, A.; Petrini, G.; Rivetti, F.; Spanò, G. *Langmuir* **1999**, *155*, 753.

(42) Bolis, V.; Bordiga, S.; Lamberti, C.; Zecchina, A.; Petrini, G.; Rivetti F.; Spanò, G. *Microporous Mesoporous Mater.* **1999**, *30*, 67.

Ti Location in Ti−Silicate-1

J. Am. Chem. Soc., Vol. 123, No. 10, 2001 2207

Table 1. First Part, Cell Volume (XRPD from Laboratory Data) and Deduced Framework Ti Content for TS-1 Coming from Syntheses A and B, Activated at 120 °C, and Sealed on a Boron Silicate Capillary and, Second Part, Neutron Data Collection Details and Rietveld Refinement Parameters Referred to the 0 Refinement Strategy[a]

XRPD from Laboratory Data on Samples Activated at 120 °C and Sealed on a Boron Silicate Capillary		
sample	A120	B120
cell vol V (Å^3)	5379.5(8)	5391.1(9)
Ti content (atoms/cell)	2.09	2.64

Neutron Data Collected on the HRPD Instrument at ISIS			
sample	A120	A500	B120
T (K)	298	298	298
ToF range (ms), 168° bank	43−118	42−118	43−118
ToF range (ms), 90° bank	35−120	35−120	36−118
cell			
a (Å)	20.1135(2)	20.0715(3)	20.1282(3)
b (Å)	19.9300(3)	19.9074(3)	19.9449(3)
c (Å)	13.4098(2)	13.3853(2)	13.4195(3)
cell vol V (Å^3)	5375.47(9)	5348.4(1)	5387.3(1)
space group	Pnma	Pnma	Pnma
tot. no. of refined params	157	157	157
Rwp	0.0229	0.0251	0.0216
Rp	0.0197	0.0218	0.0188
reduced $\chi 2$	3.325	2.383	2.450
expected Rwp	0.0126	0.0163	0.0138
R 168° bank	0.0647	0.0785	0.0485
R 90° bank	0.1206	0.1717	0.0883
tot. no. exptl points	5870	5946	5781

[a] For the definition of the quality factors we refer to the GSAS manual.[45]

the mean detectable Ti content of each site. It is worth reminding that, due to such effects, in an analogous neutron powder diffraction study aimed to detect T vacancies in defective MFI-silicalite,[44] the framework defects could be located in the orthorhombic phase (measured at room temperature) but not on the monoclinic one (measured at 100 K). For this reason we performed a preliminary temperature-dependent diffraction study at the BM16 beam line of ESRF to define the orthorhombic ⇔ monoclinic phase transition in a high-Ti-loaded TS-1 sample.[43] The transition temperature was found to occur around 160 K in the dehydrated sample, and therefore, any experiment aimed to locate the Ti atoms in the MFI framework should be performed above this temperature. We estimated that the reduction of the thermal displacement parameters expected by cooling the samples from 300 to 170 K would not yield a substantial advantage over the effective reduction of signal-to-noise ratio caused by the cryogenic equipment. Measurements were thus performed at room temperature.

IR measurements were performed on the same samples at nominally room temperature. Thin self-supporting wafers of TS-1 were prepared and activated in a vacuum at 120 °C, inside an IR cell allowing in situ measurements to be made. The IR spectra were recorded at 2 cm^{-1} resolution in transmission mode on a FTIR 2000 Perkin-Elmer equipped with MCT detector cooled at 77 K with liquid nitrogen.

3. Results and Refinement Methods

The Rietveld analysis was performed using the GSAS software system.[45] The peak profiles were modeled by a convolution of a double-exponential and a switch function[46] with a pseudo-Voigt function; the Lorentzian breadth of the peak fwhm is parametrized as $\gamma = \gamma_0 + \gamma_1 d_{hkl} + \gamma_2 d_{hkl}^2$ and the Gaussian breadth as $\sigma = \sigma_0 + \sigma_1 d_{hkl} l^2 + \sigma_2 d_{hkl}^4$. Given the large number of structural parameters, the refinement was started by

(43) Marra, G. L.; Artioli, G.; Fitch, A. N.; Milanesio, M.; Lamberti, C. *Microporous Mesoporous Mater.* **2000**, *40*, 85.

(44) Artioli, G.; Lamberti, C.; Marra, G. L. *Acta Crystallogr. B* **2000**, *56*, 2.

(45) Larson, A. C.; Von Dreele, R. B. *Report No. LAUR-68-748*; Los Alamos National Laboratory: Los Alamos, NM, 1999.

(46) Ikeda, S.; Carpenter J. M. *Nucl. Inst. Methods Phys. Res. A* **1985**, *239*, 536.
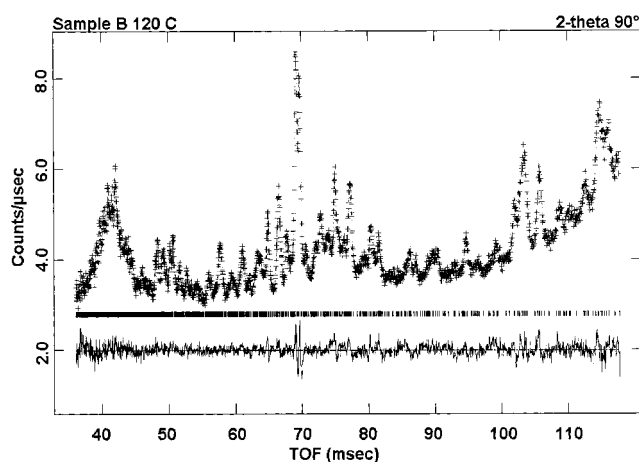

Figure 1. Observed (crosses), calculated (solid upper line), and difference (solid lower line) powder diffraction patterns for sample B120. Data from the HRPD detector bank at 90°.
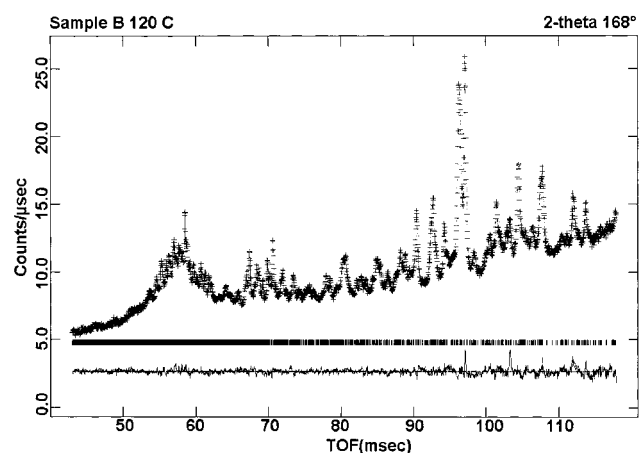

Figure 2. Observed (crosses), calculated (solid upper line), and difference (solid lower line) powder diffraction patterns for sample B120. Data from the HRPD detector bank at 168°.

imposing severe constraints on the T−O bond distances. The weights of the constraints were progressively released at convergence, being completely removed in the final cycle. Furthermore the isotropic atomic displacement parameters of all T (i.e. Si or Ti) and O sites were constrained to be equal, thus limiting the number of refined atomic displacement parameters to two. The instrumental background was modeled by a Chebyshev polynomial with 18 coefficients to refine. In the final cycles all atomic coordinates (110 parameters), 2 isotropic atomic displacement parameters, the cell parameters (resulting in a total of 115 structural parameters), 18 coefficients of the background modeling function, 1 scale factor, and 2 peak profile coefficients (σ_1 and γ_2) for each histogram (resulting in a total of 42 nonstructural parameters) were simultaneously refined. This number, 157 independent parameters, holds for the first minimization cycles, where the presence of titanium was ignored and the MFI structure of each sample was refined with the T sites fully occupied by Si atoms, hereafter labeled as refinement 0. The insertion of Ti atoms in the model implies the addition of up to 12 supplementary occupation parameters depending on the adopted refinement strategy. Detailed strategies of the refinement of site occupancy factors are discussed below.

The second part of Table 1 lists the details of the data collection and Rietveld refinements. Figures 1 and 2 show the observed, calculated, and difference powder diffraction spectra for the final refinements of the data relative to sample B120.

Table 2. Refined Atomic Fractional Coordinates, Atomic Displacement Parameters, and Average Si−O Distance or Average Si−O−Si Angle for the Three TS-1 Samples Referred to the 0 Refinement Strategy

atom	sample	x	y	z	$100U_{iso}$ (Å^2)	mean Si−O (Å)
Si(1)	A120	0.4246(5)	0.0569(5)	0.3313(6)	2.07(3)	1.596(2)
	A500	0.4255(6)	0.0550(6)	0.3325(7)	2.19(3)	1.595(2)
	B120	0.4249(6)	0.0559(6)	0.3331(6)	2.10(4)	1.595(2)
Si(2)	A120	0.3083(5)	0.0295(4)	0.1859(6)	2.07(3)	1.596(2)
	A500	0.3088(6)	0.0272(5)	0.1830(8)	2.19(3)	1.595(2)
	B120	0.3090(5)	0.0291(4)	0.1846(7)	2.10(4)	1.595(2)
Si(3)	A120	0.2779(4)	0.0612(5)	0.0336(6)	2.07(3)	1.596(2)
	A500	0.2780(5)	0.0617(5)	0.0362(7)	2.19(3)	1.595(2)
	B120	0.2779(5)	0.0621(5)	0.0338(7)	2.10(4)	1.595(2)
Si(4)	A120	0.1194(4)	0.0622(5)	0.0298(6)	2.07(3)	1.595(2)
	A500	0.1192(5)	0.0641(5)	0.0278(7)	2.19(3)	1.595(2)
	B120	0.1197(5)	0.0622(5)	0.0285(6)	2.10(4)	1.595(2)
Si(5)	A120	0.0728(5)	0.0288(4)	−0.1868(6)	2.07(3)	1.595(2)
	A500	0.0726(6)	0.0298(5)	−0.1890(7)	2.19(3)	1.595(2)
	B120	0.0723(5)	0.0289(5)	−0.1883(7)	2.10(4)	1.595(2)
Si(6)	A120	0.1893(5)	0.0616(4)	−0.3259(6)	2.07(3)	1.596(2)
	A500	0.1917(6)	0.0638(5)	−0.3240(8)	2.19(3)	1.595(2)
	B120	0.1907(5)	0.0615(4)	−0.3248(7)	2.10(4)	1.596(2)
Si(7)	A120	0.4225(5)	−0.1752(4)	−0.3222(7)	2.07(3)	1.597(2)
	A500	0.4247(7)	−0.1738(4)	−0.3252(8)	2.19(3)	1.596(2)
	B120	0.4241(6)	−0.1745(4)	−0.3232(7)	2.10(4)	1.596(2)
Si(8)	A120	0.3072(5)	−0.1294(4)	−0.1850(6)	2.07(3)	1.596(2)
	A500	0.3118(7)	−0.1325(5)	−0.1860(7)	2.19(3)	1.595(2)
	B120	0.3112(6)	−0.1302(5)	−0.1852(6)	2.10(4)	1.596(2)
Si(9)	A120	0.2729(5)	−0.1754(3)	0.0324(7)	2.07(3)	1.596(2)
	A500	0.2751(5)	−0.1748(4)	0.0333(8)	2.19(3)	1.595(2)
	B120	0.2744(5)	−0.1747(3)	0.0332(8)	2.10(4)	1.595(2)
Si(10)	A120	0.1206(5)	−0.1718(2)	0.0355(7)	2.07(3)	1.596(2)
	A500	0.1230(5)	−0.1728(3)	0.0348(8)	2.19(3)	1.595(2)
	B120	0.1219(5))	−0.1724(3)	0.0328(8)	2.10(4)	1.596(2)
Si(11)	A120	0.0702(5)	−0.1289(5)	−0.1766(6)	2.07(3)	1.596(2)
	A500	0.0725(7)	−0.1260(6)	−0.1761(7)	2.19(3)	1.595(2)
	B120	0.0721(6)	−0.1272(5)	−0.1783(7)	2.10(4)	1.596(2)
Si(12)	A120	0.1848(4)	−0.1729(3)	−0.3219(7)	2.07(3)	1.596(2)
	A500	0.1862(6)	−0.1728(3)	−0.3193(8)	2.19(3)	1.595(2)
	B120	0.1875(5)	−0.1726(3)	−0.3195(8)	2.10(4)	1.596(2)

atom	sample	x	y	z	$100U_{iso}$ (Å^2)	Si−O−Si angle (deg)
O(1)	A120	0.3778(6)	0.0483(9)	0.2361(9)	4.18(5)	151.6(11)
	A500	0.3761(7)	0.0454(9)	0.2403(10)	4.99(5)	157.9(13)
	B120	0.3775(7)	0.0456(9)	0.2391(9)	4.24(5)	155.0(12)
O(2)	A120	0.3076(8)	0.0613(7)	0.0768(6)	4.18(5)	148.6(10)
	A500	0.3070(10)	0.0606(9)	0.0747(7)	4.99(5)	149.3(13)
	B120	0.3078(8)	0.0619(7)	0.0762(6)	4.24(5)	148.3(11)
O(3)	A120	0.1987(4)	0.0652(6)	0.0283(7)	4.18(5)	174.1(9)
	A500	0.1986(5)	0.0603(8)	0.0302(8)	4.99(5)	175.9(12)
	B120	0.1989(5)	0.0662(6)	0.0274(8)	4.24(5)	173.2(10)
O(4)	A120	0.1004(5)	0.0603(7)	0.0856(6)	4.18(5)	156.8(11)
	A500	0.0986(6)	0.0622(9)	0.0873(7)	4.99(5)	156.8(14)
	B120	0.1018(6)	0.0584(9)	0.0871(7)	4.24(5)	158.5(13)
O(5)	A120	0.1172(5)	0.0560(9)	0.2767(8)	4.18(5)	147.6(10)
	A500	0.1188(7)	0.0535(11)	0.2793(9)	4.99(5)	148.9(12)
	B120	0.1183(6)	0.0512(10)	0.2792(8)	4.24(5)	149.3(11)
O(6)	A120	0.2466(6)	0.0617(8)	0.2436(9)	4.18(5)	153.6(13)
	A500	0.2488(7)	0.0623(9)	0.2411(10)	4.99(5)	152.9(14)
	B120	0.2489(7)	0.0626(8)	0.2440(10)	4.24(5)	152.9(13)
O(7)	A120	0.3753(7)	−0.1570(8)	0.2302(10)	4.18(5)	151.8(12)
	A500	0.3805(8)	−0.1613(8)	0.2279(11)	4.99(5)	145.4(13)
	B120	0.3791(8)	−0.1601(8)	0.2275(11)	4.24(5)	147.0(13)
O(8)	A120	0.3050(9)	−0.1537(5)	0.0716(6)	4.18(5)	157.8(13)
	A500	0.3069(11)	−0.1550(7)	0.0718(7)	4.99(5)	159.9(16)
	B120	0.3051(10)	−0.1545(6)	0.0723(7)	4.24(5)	161.6(15)
O(9)	A120	0.1972(5)	−0.1512(5)	0.0315(9)	4.18(5)	147.4(7)
	A500	0.1993(5)	−0.1508(6)	0.0287(11)	4.99(5)	146.3(9)
	B120	0.1985(5)	−0.1518(5)	0.0346(10)	4.24(5)	148.4(8)
O(10)	A120	0.0858(7)	−0.1616(6)	−0.0705(8)	4.18(5)	158.6(10)
	A500	0.0876(8)	−0.1593(8)	−0.0701(9)	4.99(5)	159.5(13)
	B120	0.0857(7)	−0.1593(8)	−0.0712(9)	4.24(5)	158.7(12)
O(11)	A120	0.1183(5)	−0.1515(8)	−0.2652(10)	4.18(5)	159.6(12)
	A500	0.1181(7)	−0.1555(9)	−0.2633(12)	4.99(5)	156.2(15)
	B120	0.1196(6)	−0.1564(9)	−0.2631(11)	4.24(5)	157.7(13)

Table 2 (Continued)

atom	sample	x	y	z	$100U_{iso}$ (Å^2)	Si−O−Si angle (deg)
O(12)	A120	0.2473(7)	−0.1516(8)	−0.2558(10)	4.18(5)	177.0(13)
	A500	0.2496(8)	−0.1535(9)	−0.2534(13)	4.99(5)	178.4(16)
	B120	0.2501(7)	−0.1485(9)	−0.2558(12)	4.24(5)	174.5(13)
O(13)	A120	0.3171(6)	−0.0500(4)	−0.1895(8)	4.18(5)	165.9(9)
	A500	0.3163(7)	−0.0526(5)	−0.1874(9)	4.99(5)	170.9(11)
	B120	0.3169(7)	−0.0505(4)	−0.1896(9)	4.24(5)	169.1(11)
O(14)	A120	0.0810(6)	−0.0498(4)	−0.1675(9)	4.18(5)	160.6(9)
	A500	0.0844(7)	−0.0474(5)	−0.1619(10)	4.99(5)	153.6(11)
	B120	0.0820(7)	−0.0486(5)	−0.1624(10)	4.24(5)	155.2(10)
O(15)	A120	0.4147(7)	0.1298(6)	−0.3782(10)	4.18(5)	145.0(10)
	A500	0.4141(9)	0.1253(7)	−0.3870(12)	4.99(5)	152.5(12)
	B120	0.4157(8)	0.1262(6)	−0.3883(11)	4.24(5)	150.6(12)
O(16)	A120	0.4105(7)	0.0023(7)	−0.4160(9)	4.18(5)	160.0(12)
	A500	0.4119(9)	−0.0013(7)	−0.4148(11)	4.99(5)	161.9(15)
	B120	0.4123(8)	0.0016(7)	−0.4184(11)	4.24(5)	157.8(13)
O(17)	A120	0.3977(7)	−0.1304(7)	−0.4137(10)	4.18(5)	155.4(11)
	A500	0.4011(9)	−0.1339(7)	−0.4224(11)	4.99(5)	148.3(12)
	B120	0.3991(8)	−0.1298(7)	−0.4145(11)	4.24(5)	156.1(12)
O(18)	A120	0.1912(9)	0.1312(5)	−0.3843(8)	4.18(5)	146.8(11)
	A500	0.1883(9)	0.1346(6)	−0.3795(9)	4.99(5)	139.8(12)
	B120	0.1915(10)	0.1323(5)	−0.3800(9)	4.24(5)	144.4(12)
O(19)	A120	0.1951(9)	0.0012(6)	−0.4036(8)	4.18(5)	163.0(13)
	A500	0.2005(10)	0.0016(6)	−0.3982(9)	4.99(5)	169.9(15)
	B120	0.1996(9)	0.0015(6)	−0.4024(8)	4.24(5)	167.8(13)
O(20)	A120	0.1990(9)	−0.1317(6)	−0.4217(8)	4.18(5)	145.1(9)
	A500	0.1964(11)	−0.1317(7)	−0.4205(9)	4.99(5)	143.0(11)
	B120	0.1998(10)	−0.1325(7)	−0.4206(9)	4.24(5)	144.2(10)
O(21)	A120	−0.0027(5)	0.0453(8)	−0.2132(9)	4.18(5)	145.1(9)
	A500	−0.0020(6)	0.0508(10)	−0.2158(10)	4.99(5)	141.2(10)
	B120	−0.0026(5)	0.0489(9)	−0.2136(10)	4.24(5)	143.4(9)
O(22)	A120	−0.0017(5)	−0.1579(8)	−0.2022(11)	4.18(5)	154.2(10)
	A500	−0.0020(7)	−0.1484(10)	−0.2013(11)	4.99(5)	154.9(12)
	B120	−0.0010(6)	−0.1539(9)	−0.2014(11)	4.24(5)	156.4(11)
O(23)	A120	0.4250(13)	−0.25	−0.3646(14)	4.18(5)	138.1(15)
	A500	0.4214(16)	−0.25	−0.3619(18)	4.99(5)	143.8(18)
	B120	0.4220(15)	−0.25	−0.3623(16)	4.24(5)	141.5(17)
O(24)	A120	0.1987(11)	−0.25	−0.3460(12)	4.18(5)	148.9(14)
	A500	0.1963(15)	−0.25	−0.3473(14)	4.99(5)	149.0(16)
	B120	0.1993(13)	−0.25	−0.3440(13)	4.24(5)	150.6(15)
O(25)	A120	0.2884(9)	−0.25	0.0689(12)	4.18(5)	137.4(12)
	A500	0.2876(11)	−0.25	0.0699(14)	4.99(5)	139.6(15)
	B120	0.2862(10)	−0.25	0.0693(13)	4.24(5)	140.4(14)
O(26)	A120	0.1155(11)	−0.25	0.0596(15)	4.18(5)	155.5(15)
	A500	0.1166(13)	−0.25	0.0652(17)	4.99(5)	148.9(17)
	B120	0.1169(11)	−0.25	0.0611(16)	4.25(5)	151.5(16)

The systematic discrepancy between the cell volume observed by neutrons (present study) and by X-rays[12] [5379.5(8) vs 5375.4(9) Å^3 for sample A120 and 5391.1(9) vs 5387.3(1) Å^3 for sample B120] can be explained by taking into account the larger volume of sample needed for neutron measurements (about 3 cm^3) with respect to the volume used for XRPD. It is plausible that a small difference in the degree of dehydration has been reached in the two cases and this may be the origin of the small (about 4 Å^3) volume contraction observed by neutron diffraction. Anyway this small effect bears no consequences on the location of the Ti atoms.

The refined atomic coordinates and isotropic thermal parameters of TS-1 structures are reported in Table 2, together with the mean tetrahedral distances and T−O-T angles, 0 refinement level. The full list of interatomic distances and angles is available from the authors upon request.

Despite the substantial contrast between the Si and the Ti neutron coherent scattering lengths, refinement of the tetrahedral site occupancy factors (sof's) is always critical because of severe correlation between scale factors, sof's, and atomic displacement parameters during the least-squares minimization procedure. The issue is further complicated by the low Ti-content inserted in the MFI framework. To assess the bias imposed on the results

by parameter correlation, it was decided to test the presence of Ti on the symmetry-independent T sites by adopting different refinement strategies and then critically compare the results independently derived from each data set. A similar approach was adopted before.[12,43,44]

The MFI structure of each sample was first refined with the T sites fully occupied by Si atoms, refinement 0. Only two independent atomic displacement parameters (adp) were optimized, one for the 12 T sites and another for the 26 oxygen atoms. Once the MFI structure was fully optimized, then the presence of Ti atoms on T sites was checked using five different refinement strategies labeled in the following as methods a−e. Method a: The previously refined isotropic adp for the tetrahedral sites was kept fixed, and the sof's of all T sites were simultaneously refined by assuming full site occupancy (Si + Ti = 1.0) and no limitation on the total Ti content. Method b: The sof's of the sites resulting in a negative Ti content from the previous refinement (method a) were reset to Ti = 0.0 and fixed to Si = 1.0. The sof's of the remaining T sites were refined assuming no limitation on the total Ti content, being adp fixed as in method a. Method c: Starting from the MFI fully optimized structure, the sof's of all T sites were simultaneously refined together with the adp, constraining the total Ti content to

Table 3. Site Occupancy Parameters (Sof's) Obtained by Adopting Different Refinement Strategies[a]

sample/strategy	T1	T2	T3	T4	T5	T6	T7	T8	T9	T10	T11	T12	Ti (tot.)
B120 C (a)	−0.04(2)	0.01(2)	0.03(2)	−0.01(2)	−0.05(2)	0.17(2)	0.12(3)	0.02(2)	0.01(2)	0.08(2)	0.21(2)	−0.06(2)	
B120 C (b)	0.00(0)	−0.02(2)	0.03(2)	0.00(0)	0.00(0)	0.14(2)	0.07(2)	0.02(2)	0.00(2)	0.07(2)	0.21(2)	0.00(0)	4.16
B120 C (c)	0.03(2)	0.00(2)	0.02(2)	0.02(2)	0.01(2)	0.05(2)	0.04(2)	0.04(2)	0.01(3)	0.02(2)	0.07(1)	0.02(2)	2.62
B120 C (d)	0.00(0)	0.00(0)	0.00(0)	0.00(0)	0.00(0)	0.09(1)	0.07(1)	0.06(2)	0.00(0)	0.00(0)	0.11(1)	0.00(0)	2.64
B120 C (e)	0.00(0)	0.00(0)	0.03(2)	0.00(0)	0.00(0)	0.09(1)	0.06(2)	0.00(0)	0.00(0)	0.04(2)	0.11(1)	0.00(0)	2.62
A120 C (a)	−0.06(2)	0.04(2)	0.12(2)	−0.08(2)	−0.04(2)	0.19(2)	0.06(2)	−0.06(2)	−0.10(2)	0.19(2)	0.25(2)	0.00(2)	
A120 C (b)	0.00(0)	0.01(1)	0.05(2)	0.00(0)	0.00(0)	0.16(1)	0.03(2)	0.00(0)	0.00(0)	0.13(2)	0.22(2)	0.00(0)	3.92
A120 C (c)	0.02(2)	0.01(2)	0.01(2)	0.01(2)	0.01(2)	0.04(1)	0.03(2)	0.02(2)	0.01(2)	0.03(2)	0.05(1)	0.02(2)	2.11
A120 C (d)	0.00(0)	0.00(0)	0.00(0)	0.00(0)	0.00(0)	0.08(1)	0.04(2)	0.00(0)	0.00(0)	0.05(2)	0.09(1)	0.00(0)	2.09
A120 C (e)	0.00(0)	0.00(0)	0.03(2)	0.00(0)	0.00(0)	0.08(1)	0.04(2)	0.00(0)	0.00(0)	0.04(2)	0.08(1)	0.00(0)	2.10
A500 C (a)	−0.03(2)	0.02(2)	0.07(2)	0.00(2)	−0.03(2)	0.14(2)	0.13(2)	0.03(2)	0.01(3)	0.10(3)	0.15(2)	−0.02(3)	
A500 C (b)	0.00(0)	0.00(2)	0.08(2)	0.00(0)	0.00(0)	0.14(2)	0.11(2)	0.04(2)	−0.00(2)	0.13(2)	0.17(2)	0.00(0)	5.36
A500 C (c)	0.02(2)	0.00(2)	0.02(2)	0.02(2)	0.00(3)	0.04(2)	0.03(2)	0.03(2)	0.01(3)	0.03(3)	0.05(2)	0.02(3)	2.10
A500 C (d)	0.00(0)	0.00(0)	0.00(0)	0.00(0)	0.00(0)	0.08(1)	0.06(2)	0.06(2)	0.00(0)	0.00(0)	0.06(2)	0.00(0)	2.10
A500 C (e)	0.00(0)	0.00(0)	0.04(2)	0.00(0)	0.00(0)	0.08(1)	0.06(2)	0.00(0)	0.00(0)	0.03(2)	0.06(2)	0.00(0)	2.10

[a] The last column reports the total Ti content (in Ti atoms/unit cell) resulted from the refinement.

Table 4. Total Number of Free Parameters (*N*) and Quality Factors of the Fit for the Different Refinement Strategies Adopted on the Three Samples[a]

sample/strategy	N	Rwp	Rp	reduced χ^2	expected Rwp
B120 (a)	167	0.0207	0.0178	2.266	0.0138
B120 (b)	163	0.0207	0.0178	2.268	0.0137
B120 (c)	169	0.0209	0.0181	2.312	0.0137
B120 (d)	161	0.0208	0.0180	2.289	0.0137
B120 (e)	162	0.0208	0.0180	2.294	0.0137
A120 (a)	167	0.0216	0.0182	2.959	0.0126
A120 (b)	164	0.0217	0.0182	2.980	0.0126
A120 (c)	169	0.0221	0.0187	3.121	0.0125
A120 (d)	161	0.0220	0.0187	3.084	0.0125
A120 (e)	161	0.0220	0.0187	3.085	0.0125
A500 (a)	167	0.0239	0.0202	2.159	0.0163
A500 (b)	165	0.0235	0.0201	2.096	0.0162
A500 (c)	169	0.0241	0.0205	2.206	0.0162
A500 (d)	161	0.0243	0.0208	2.227	0.0163
A500 (e)	162	0.0243	0.0208	2.238	0.0162

[a] For the definition of the quality factors we refer to the GSAS manual.[45]

chemical analysis value, that is 2.09 atoms/cell for samples A120 and A500 and 2.64 atoms/cell for sample B120. Method d: The sof's of only the most populated T sites (above 1σ level as resulted from method c) were simultaneously refined together with the adp, constraining again the Ti content to the chemical analysis value. Method e: Again the sof's of only the most populated T sites in method b were simultaneously refined together with the adp, imposing chemical constrains on total Ti value. In methods c−e the starting values for Ti fractions in the T sites are those obtained by equally distributing the total Ti amount among the sites involved. The sof's resulting from the different refinements are listed in Table 3, while the total number of independent parameters, which is refinement dependent, and the fit quality factors for each refinement are reported in Table 4.

4. Discussion

Since the total amount of Ti substitution is rather low, a strong correlation between sof's and atomic displacement parameters is always present, so that we cannot be fully confident on the results of a single refinement strategy. The only chance is to critically compare the results obtained by different refinement procedures. We realize that this approach is a very restrictive one and has two main disadvantages: (i) It is extremely time-consuming. (ii) Some "slightly preferred" sites may be over-looked. On the contrary, it has the important advantage that the accepted sites, if any, are to be considered with confidence.

Table 5 reports the site occupancy factors of the sites mostly populated by Ti atoms, using the corresponding esd as units. Perusal of the table clearly indicates that only a few sites appear to be consistently occupied by Ti atoms within a few standard deviations. Sites T6, T7, and T11 show a substantial amount of Ti atoms in all three samples independently of the adopted refinement strategy. Such sites are always significantly occupied by Ti at the 2−12σ level, and even by a limiting of the maximum allowed Ti content (methods c−e), all these sites are occupied at least at the 2−7σ level. Site T10 shows an anomalous behavior, displaying a substantial Ti content only for the first two strategies of refinement. When chemical constrains are applied, the Ti fraction in T10 is not significant, and it does not exceed the 1−2σ level. T3 and T8 always show a Ti content barely within significance, constantly within the 1−2σ level. This behavior seems to be sample dependent, and the two sites are hardly to be considered occupied by Ti atoms. Sites T1, T2, T4, T5, T9, and T12 do not show sign of Ti occupancy in any of the samples as their fraction values are either negative or close to zero within the 1σ level. These sites have been excluded from Table 5 as it is assumed that Ti has no preference for such sites.
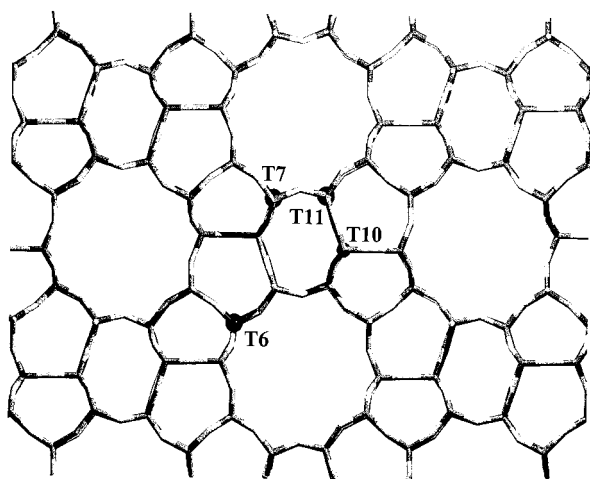
The fact that the very same sites (T6, T7, T11) are found to contain a significant fraction of Ti atoms, independently of the refinement strategy and independently of the sample preparation and treatment, grants some confidence in the results, which should of course be taken with caution if obtained from an isolated structure refinement. Figure 3 reports the MFI framework, where the positions of sites T6, T7, T11, and T10 have been evidenced.

4.1. Comparison with Low-Temperature Synchrotron Radiation XRPD Data. In a recent work[43] we reported the attempt to locate Ti in a high Ti-loaded TS-1 sample using low-temperature XRPD data collected at the BM16 beam line of ESRF. The refinement of the data yields weak evidence that (i) T11 and T10 are probably the most populated sites, (ii) sites T4 and T12 seem not to be occupied at all by Ti, and (iii) nothing significant could be said for the remaining T1, T2, T3, T5, T6, T7, T8, and T9 sites. Given the lower sensibility of X-rays in the discrimination between Si and Ti with respect to neutrons, the above results i and ii are in remarkable agreement with the neutron results presented here.

4.2. Comparison with Neutron Diffraction of Ti-Free Silicalite and Hypothesis on the Insertion Mechanism of Ti in the MFI Framework. In an ongoing research work described in several papers[41,42,44,47,48] our group has evidenced that Ti-
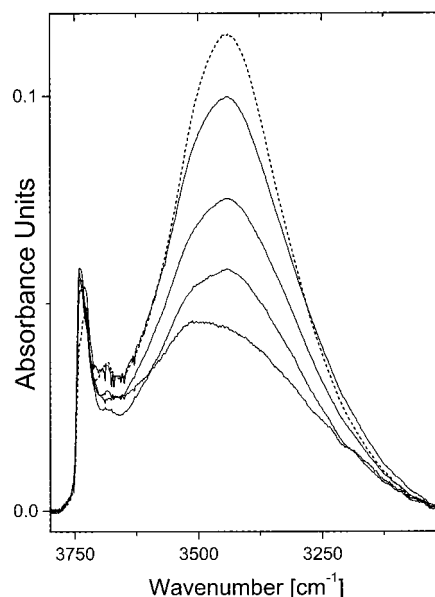
Table 5. Comparison of the Refined Values of the Sof of the Most Populated Sites, Measured Using the Corresponding Esd as Unit, as a Function of the Different Refinement Strategies Applied on the Three TS-1 Samples

sites	sample strategy	B120C					A120C					A500C				
		a	b	c	d	e	a	b	c	d	e	a	b	c	d	e
T6		8σ	7σ	2σ	6σ	6σ	8σ	10σ	3σ	5σ	6σ	7σ	7σ	2σ	6σ	6σ
T7		4σ	3σ	2σ	5σ	3σ	3σ	σ	2σ	2σ	2σ	6σ	5σ	σ	3σ	3σ
T11		10σ	10σ	5σ	7σ	7σ	12σ	11σ	3σ	6σ	6σ	7σ	8σ	2σ	3σ	3σ
T10		4σ	3σ	σ	0	2σ	9σ	6σ	σ	2σ	2σ	3σ	6σ	σ	0	σ
T3		σ	σ	σ	0	σ	6σ	2σ	0	0	σ	3σ	4σ	σ	0	2σ
T8		σ	σ	2σ	3σ	0	0	0	σ	0	σ	σ	2σ	σ	3σ	0

Figure 3. Stick representation of the MFI orthorhombic structure, viewed along the [010] direction. T sites and oxygen atoms have been represented by dark and clear sticks, respectively. The preferentially substituted T6, T7, and T11 sites have been evidenced by big black spheres, while for T10 a smaller black sphere has been used. For clarity, the symmetry operations have not been applied to such spheres.

free silicalite, synthesized according to the original patent for TS-1 (i.e. just without including TiO₂ in the reactants), is a defective material showing a high density of framework Si vacancies resulting in hydroxylated nests. In a previous neutron diffraction study[44] we showed that Si vacancies do not occur randomly and they are preferentially hosted in the Si(6), Si(7), Si(11), and Si(10) sites.

The correspondence of the four sites preferentially hosting the Si vacancies in defective silicalite with those preferentially occupied by Ti atoms in TS-1 is striking. Moreover, it has been shown using several independent characterization techniques[19,22,24–42] (IR, UV–vis, EXAFS, microcalorimetry, and others) that the insertion of the Ti heteroatoms in the MFI lattice has a mineralizing effect, causing the progressive reduction of the framework defects. Figure 4 reports the OH stretching region of the IR spectra of TS-1 samples activated at 120 °C and having increasing Ti content in the range 0 (silicalite) to 2.64 atoms/unit cell. On the basis of the IR spectra, it is evident that the

(47) Zecchina, A.; Bordiga, S.; Spoto, G.; Marchese, L.; Petrini, G.; Leofanti, G.; Padovan, M. *J. Phys. Chem.* **1992**, *96*, 4985. Zecchina, A.; Bordiga, S.; Spoto, G.; Marchese, L.; Petrini, G.; Leofanti, G.; Padovan, M. *J. Phys. Chem.* **1992**, *96* 4991. Zecchina, A.; Bordiga, S.; Spoto, G.; Marchese, L.; Petrini, G.; Leofanti, G.; Padovan, M.; Otero Areàn, C. *J. Chem. Soc., Faraday Trans.* **1992**, *88*, 2959. Bordiga, S.; Ricchiardi, G.; Lamberti, C.; Scarano, D.; Spoto, G.; Zecchina, A. *Mater. Eng.* **1994**, *5*, 197. Marra, G. L.; Tozzola, G.; Leofanti, G.; Padovan, M.; Petrini, G.; Genoni, F.; Venturelli, B.; Zecchina, A.; Bordiga, S.; Ricchiardi, G. *Stud. Surf. Sci. Catal.* **1994**, *84*, 559.

(48) Bordiga, S.; Roggero, I.; Ugliengo, P.; Zecchina, A.; Bolis, V.; Artioli, G.; Buzzoni, R.; Marra, G. L.; Rivetti, F.; Spanò, G.; Lamberti, C. *J. Chem. Soc., Dalton Trans.* **2000**, 3921. (b) Bordiga, S.; Ugliengo, P.; Damin, A.; Lamberti, C.; Spoto, G.; Zecchina, A.; Spanò, G.; Buzzoni, R.; Dalloro, L.; Rivetti, F. *Top. Catal.*, in press.

Figure 4. IR spectra, in the OH stretching region, of, from top to bottom, TS-1 samples (full line spectra) with increasing Ti content, from 0 (silicalite, dashed spectrum) to 2.64 atoms/unit cell. All samples have been activated at 120 °C.

progressive incorporation of Ti atoms in the framework implies the parallel reduction of the OH band due to internal, defective, Si–OH groups.

The combined crystallographic evidence (obtained on defective silicalites and on TS-1) together with the mineralizing effect of Ti heteroatoms strongly suggests that the incorporation mechanism of the Ti atoms in the MFI framework occurs via the insertion of titanium in defective sites of silicalite. In this context, it is worth reminding that the simulation results of Ricchiardi et al.[34] indicate that the [TiO₄] and the [(OH)₄] units substituting regular [SiO₄] units in the MFI framework of silicalite have a rather similar size. This can explain the tendency of the same sites to host either a defect (Si vacancy) or a Ti heteroatom. This also explains why the amount of incorporated Ti increases to the detriment of internal OH species. The fact that three out of the four preferential T sites, for both Ti insertion and Si vacancy, are adjacent to each other [T(7)–O(35)–T(7), T(7)–O(34)–T(11), T(10)–O(22)–T(11), T(10)–O(38)–T(10)] implies that, in principle, a fraction of Ti atoms could be located in proximity of a Si vacancy. So, the whole picture emerging from the combined neutron diffraction and IR study (on TS-1 samples in the 0–2.64 Ti atoms/unit cell range) suggests that, beside regular [Ti(OSi)₄] sites, also defective [Ti(OSi)₃OH] sites could be significantly present, supporting what is already hypothesized by some authors on the basis of different characterization techniques.[19,22,24,25,41,42]

4.3. Comparison with Data or Calculations on the Insertion of Al(III) and Fe(III) in the MFI Framework. As far as the aluminum insertion in MFI structures (ZSM-5) is concerned,

it may be reminded that the problem has been debated in the theoretical works of Redondo and Hay,[49] Kramer and van Santen,[50] and Ricchiardi and Newsam.[51] In all cases the authors have predicted a uniform distribution of Al. The fact that Al and Si differ by only one electron discards any attempt to directly locate Al by XRPD measurements. Very recently, Olson et al.[52] have highlighted (by Rietveld refinement of synchrotron X-ray diffraction data) that Cs^+ cations in Cs-ZSM-5 are located in three different extraframework sites. From this evidence they conclude that framework sites T4, T7, T10, T11, and T12, being connected with oxygen atoms exhibiting a O−Cs distance less than 3.55 Å, are good candidates for hosting Al atoms. On the contrary, insertion of Al in T2, T8, and T9 sites is less probable, owing to too high O−Cs distances: always higher than 3.90 Å.

Concerning Fe−silicalite, Eckert et al. have presented at the XVIII IUCr Congress (Glasgow, 4-13 Aug 1999) a neutron powder diffraction study indicating that the T8 site is a preferential site for Fe. This result disagrees with the single-crystal X-ray diffraction study based on data collected at the BM1 line of ESRF by Milanesio et al.[53] In that work sites T9 and T10 are considered as the most probable substitution sites because (i) they are located close to the extraframework Na^+ cation sites, (ii) there is the significant lengthening of the T9-O and T10-O distances, (iii) a residual electron density of 0.34 e/Å^3 and of 0.19 e/Å^3 is present at sites T9 and T10, respectively, and (iv) they show the maximum anisotropy in the thermal displacement parameters, which is a typical effect related to site substitution. It is interesting to note that T sites showing the minimum T−O distances in Fe−silicalite are T2, T4, T5, and T12,[53] and such sites do not show any tendency to incorporate Ti (see Table 4). Unfortunately the present neutron powder data do not support the determination of the T−O distances with a sensibility down to 0.005 Å; as a consequence, no meaningful correlation between sof's and T−O distances can be presented.

5. Conclusions

We report the first direct evidence that Ti atoms are not equally distributed in the MFI structure. The most populated sites are T6, T7, and T11, and weaker evidence has been found for T10. Sites T1, T2, T4, T5, T9, and T12 do not show sign of Ti occupancy, while for the remaining sites there is no conclusive evidence. These results are in good agreement with the indirect finding obtained by microcalorimetry by Bolis et al.[41,42] Four concomitant facts have contributed to this successful experimental result: (i) the preparation of a large volume of high-quality TS-1 samples with the highest possible Ti content, performed in the EniChem laboratories; (ii) the use of neutron diffraction, having a much higher scattering contrast between Ti and Si with respect to X-rays; (iii) the use of a state-of-the-art powder instrument (HRPD) having virtually the best presently available resolution in d-space; (iv) the preliminary temperature-dependent X-ray diffraction study performed at the BM16 beam line of ESRF.[43] To avoid any bias during the structure analysis, three TS-1 samples have been measured and five different refinement strategies have been adopted.

The striking coincidence that defective silicalite exhibits the same preferential sites (T6, T7, T11, and T10) for Si vacancies[44]

allows us to speculate that the incorporation mechanism of the Ti atoms in the MFI framework occurs via the insertion of titanium in defective sites of silicalite. This hypothesis agrees with the well-known mineralizing effect that titanium has on the MFI framework, and it is supported by several independent spectroscopic data on both TS-1 and defective silicalite.[19,22,24−42,44,47,48]

Note Added in Proof: After the submission of our manuscript, an interesting paper appeared in the last 2000 issue of *J. Phys. Chem. B*.[54] The authors report a neutron diffraction study on one Fe−silicate and three TS-1 samples. In agreement with the present results, on TS-1, and with the study of Milanesio et al.,[53] also Hijar et al. report evidence on a nonrandom distribution of both heteroatoms. In particular, the authors suggest T8 as preferential substitution sites for iron in Fe−silicalite and T3, T7, T8, T10, and T12 for titanium in TS-1. As far as TS-1 is concerned, it is evident that the agreement between the results reported in ref 54 and those reported here is only partial (both groups suggest T7 and T10). We can just stress that, in the present work, we give a more detailed description of all problems inherent to the data analysis and we have gone to great lengths to avoid getting biased results. Moreover, it is worth underlining that the whole picture emerging from the combined neutron diffraction and IR study on both TS-1 and defective silicalite strongly validates our conclusions. Hijar et al. also reported a computational study aimed to investigate the differences in energy gain induced by insertion of Ti in the 12 T sites. The results of the computation did not show any correlation between the energetically most stable sites and those claimed to have the higher experimental Ti occupancy. They suggested that the disagreement between computational and experimental results could be due to kinetics of framework formation. However, the quality of the calculations used may also be insufficient to handle such a complex problem. In fact, the computational method adopted (semiempirical PM3) is rather low with respect to the state of the art (see e.g. ref 34). Also the use of a bare cluster model (without embedding) can be questionable in the study of periodic systems. Unfortunately, the reported calculations cannot be reproduced since the parameters used for Ti are not yet available in the literature. In any case, a computed Ti−O distance of 1.85 Å is definitively too large (see Introduction).

Supporting Information Available: Three X-ray crystallographic files (CIF) related to the refinement strategies (b) for samples A120, B120, and A500. This material is available free of charge via the Internet at http://pubs.acs.org.

JA003657T

(49) Redondo, A.; Hay, P. J. *J. Phys. Chem.* **1993**, *97*, 11754.
(50) Kramer G. J.; van Santen, R. A. *J. Am. Chem. Soc.* **1993**, *115*, 2887.
(51) Ricchiardi, G.; Newsam, J. M. *J. Phys. Chem. B* **1997**, *101*, 9943.
(52) Olson, D. H.; Khosrovani, N.; Peters, A. W.; Toby, B. H. *J. Phys. Chem. B* **2000**, *104*, 4844.
(53) Milanesio, M.; Lamberti, C.; Aiello, R.; Testa, F.; Piana, M.; Viterbo, D. *J. Phys. Chem. B* **2000**, *104*, 9951.
(54) Hijar, C. A.; Jacubinas, R. M.; Eckert, J.; Henson, N. J.; Hay, P. J.; Ott, K. C. *J. Phys. Chem. B* **2000**, *104*, 12157.